

Research Article

Cindy Goppold*, Thomas Pinder and Patrick Herwig

Transient beam oscillation with a highly dynamic scanner for laser beam fusion cutting

DOI 10.1515/aot-2015-0059

Received December 2, 2015; accepted January 13, 2016; previously published online February 4, 2016

Abstract: Sheet metals with thicknesses >8 mm have a distinct cutting performance. The free choice of the optical configuration composed of fiber diameter, collimation, and focal length offers many opportunities to influence the static beam geometry. Previous analysis points out the limitations of this method in the thick section area. Within the present study, an experimental investigation of fiber laser fusion cutting of 12 mm stainless steel was performed by means of dynamical beam oscillation. Two standard optical setups are combined with a highly dynamic galvano-driven scanner that achieves frequencies up to 4 kHz. Dependencies of the scanner parameter, the optical circumstances, and the conventional cutting parameters are discussed. The aim is to characterize the capabilities and challenges of the dynamic beam shaping in comparison to the state-of-the-art static beam shaping. Thus, the trials are evaluated by quality criteria of the cut edge as surface roughness and burr height, the feed rate, and the cut kerf geometry. The investigation emphasizes promising procedural possibilities for improvements of the cutting performance in the case of fiber laser fusion cutting of thick stainless steel by means of the application of a highly dynamic scanner.

Keywords: beam shaping; dynamic; intensity distribution; laser fusion cutting; oscillation.

1 Introduction

The market for laser material processing is divided into micro and macro applications. The global market growth for laser systems for material processing was 8% in 2014 with a net worth of up to US\$11.6 billion. The macro range has a share of about three quarters. Both appropriate technologies, high-power laser beam cutting and welding, had the strongest economic expansion next to the precision processing from the micro sector. Main revenues were generated in the metal sector. The sales figures of the laser machine manufacturers prove that the solid state lasers are comparable to the CO₂ laser sources [1–7]. Since the beginning of the 21st century, many researchers published the advantages of solid state lasers against CO₂ lasers for the range of thin sheet cutting as well as the present challenges for thicker materials [8–24].

The approaches to improve the cut quality from the fiber laser are manifold, but the idea is always to adjust the spatial intensity distribution of the laser spot to the demanded application. The geometrical properties could be influenced as well as the intensity distribution itself. Both procedures belong to the static beam shaping methods, which means that the beam is modified before the machining process starts. An advantage of a uniform intensity distribution is the sharp edge of the focus spot, which creates a high-defined transition between treated and untreated zones. The so-called ‘top-hat shaper’ consists of refractive or diffractive optics [25–27]. Another possibility is the geometrical modification of the laser beam shape. Imaginable solutions for the cutting branch would be to change the optical setup to utilize different beam dimensions [9, 24], separate single beams into patterns [28, 29], or generate two focal spots in one beam [30]. An optical configuration that creates a larger focal spot is commonly discussed to improve the cutting performance for thicker sheets [31]. This method increases the interaction zone of the laser beam and material surface, but limits the achievable intensity. The optical setup is the minor influencing factor of the cutting performance for 15 mm-thick stainless steel plates at a steady power level

*Corresponding author: Cindy Goppold, Fraunhofer IWS, Winterbergstraße 28, 01277 Dresden, Germany, e-mail: cindy.goppold@iws.fraunhofer.de

Thomas Pinder and Patrick Herwig: Fraunhofer IWS, Winterbergstraße 28, 01277 Dresden, Germany

[32]. One suggestion is that heat conduction is the limiting factor on the maximum cutting rates [28]. A recommendation is the utilization of beam oscillation to obtain quasi-static heat conduction, meaning: the relaxation time of the atoms is higher than the required time for one oscillation period [31].

Beam oscillation is a dynamic method of beam shaping, which implies a superimposed modification of the beam regarding the feed direction during the process. Thus, the beam oscillates around the generated cut kerf and, thereby, shapes the interaction zone into an arbitrary geometry. A main advantage is the maintained intensity distribution of the fiber laser beam because every influence on the process is performed by the spatial and temporal modification of the energy deposition. Two of the most noted applications for beam shaping through oscillation are the electron beam welding [33–35] and laser beam welding [33, 36–42]. Cutting applications have been investigated for flame cutting [43–45] and fusion cutting [46, 47]. The dynamic beam shaping in the case of the laser beam fusion cutting were compared with conventional static beam shaping. The results highlight the beam oscillation as a promising method to improve the cutting performance of fiber laser for the thick material range [47]. The present investigation aims to continue the comparison of the concept of dynamic beam shaping via fast-moving mirrors and the static beam shaping with rigid lenses. The basis is a comprehensive cutting series of two optical configurations. Furthermore, dependencies of the scanner parameters and the conventional cutting parameters will be outlined.

2 Experimental procedure

Laser fusion cutting experiments were performed with a fiber laser at a $1.07\ \mu\text{m}$ wavelength. A laser output power of 3 kW and a randomly polarized beam were utilized for all investigations, as well as a conical gas nozzle and nitrogen as an assist gas. Stand-off distance between nozzle and sheet surface was kept constant. Figure 1 represents the general setup of the experiment. The chosen optical setups are standard configurations for laser fusion cutting, on the one hand of thin metal sheets and, on the other hand for thick plates. Both are summarized in Table 1. Stainless steel sheets AISI 304 (1.4301) with a thickness of 12 mm were applied as a work piece. The specifications of the scanner are outlined in Table 2. The oscillation movement is characterized by the *Lissajous* figure. In turn, this pattern is described by the frequency and amplitude for both mirrors in the X- and Y-direction, as well as the phase shift φ that defines the positioning offset of the two oscillatory motions. These additional five scanner parameters interact with the conventional cutting parameters as focal plane, feed rate, gas pressure, etc.

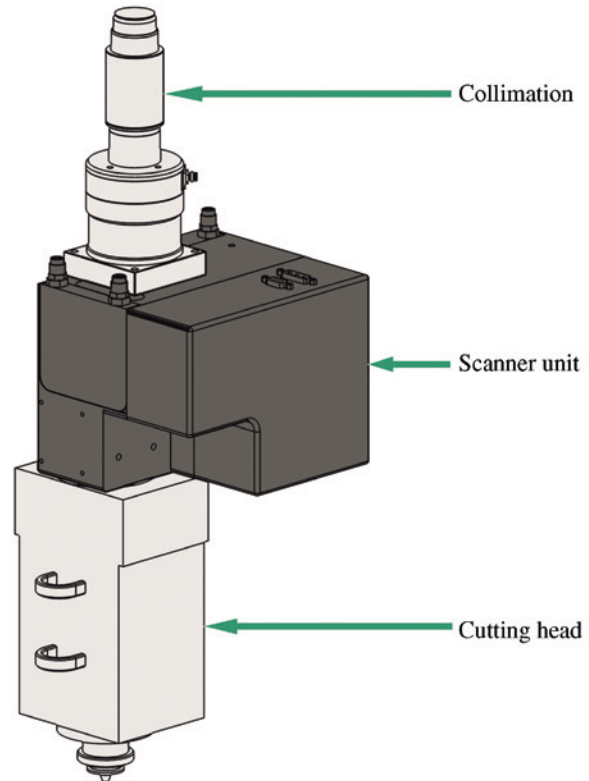


Figure 1: Schematic construction of the setup.

Table 1: Laser beam parameters.

Beam parameters	Setup 1	Setup 2
Used output power P	3 kW	
Fiber diameter d	100 μm	
Collimation length f_{col}	100 mm	
Focus length f_{foc}	125 mm	200 mm
Focus radius w_0 (86%)	59 μm	97 μm
Rayleigh length z_R	1.1 mm	3 mm
Beam quality factor M^2	9.1	

Table 2: Specifications of the scanner.

Scanner parameters	Data
Maximum amplitude (at 2 kHz sinus)	3.1 mrad
Typical speed	40 rad/s
Maximum speed	50 rad/s
Repeatability	<22 μrad

The aim of the cutting experiments was to determine the best cut edge quality at maximum reachable cutting speeds for selected scanner parameter combination. The main criteria for cut quality are the absence of burr and a homogenous, smooth appearance of the cut edge. Evaluation of the cut was performed via roughness measurements of the cut edge according to DIN EN ISO 4288:1998-04 at three positions on each cut edge – 1 mm below the upper cut edge, half of

the sheet thickness, and 1 mm above the lower cut edge and is depicted in Figure 2. To assess the surface roughness, a classification was used, as depicted in Table 3. Furthermore, an inspection of the burr was accomplished. The metrology is refined and, thus, the levels deviating from Goppold et al. [47]. The cut length of the sample is divided into five sections in which the maximum burr height is detected separately by image processing as illustrated in Figure 3. The average burr height is determined referring to the calculation of the surface roughness R_z as seen in equation 1. The classification of the burr levels in Table 4 depends upon the Gaussian distribution of the measured burr heights in its entirety.

$$\text{burr}_{\text{average}} = \frac{1}{5} \sum_{i=1}^5 \text{burr}_{\text{max}}(i) \tag{1}$$

The last evaluation step is the so-called performance, a combination of the single normalized criteria surface roughness, burr, and the

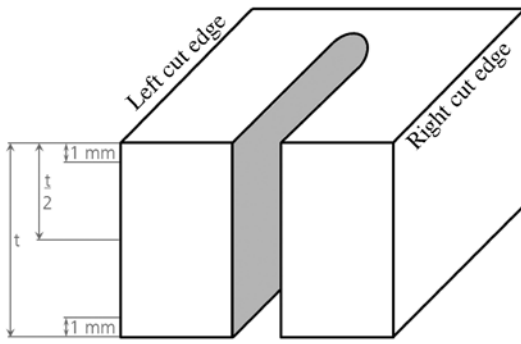


Figure 2: Scheme of the surface roughness measurement.

Table 3: Classification of the surface roughness criterion.

	Mean value $R_z \leq 50 \mu\text{m}$	Mean value $R_z \geq 50 \mu\text{m}$
Standard deviation $R_z \leq 20 \mu\text{m}$	1	3
Standard deviation $R_z \geq 20 \mu\text{m}$	2	4

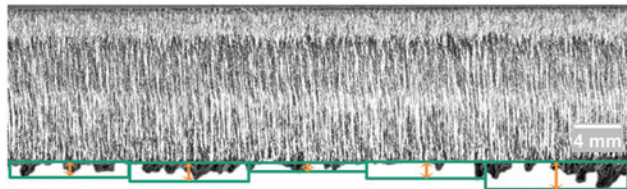


Figure 3: Scheme of the burr measurement.

Table 4: Classification of the burr criterion.

Level	Height of burr (mm)
1	$x_{\text{max}} \leq 0.5$
2	$0.5 < x_{\text{max}} \leq 1.0$
3	$x_{\text{max}} > 1.0$

achieved cutting speed v_c . The empirically ascertained calculation in the case of laser fusion cutting can be seen in equation 2. The smaller the resulting value is, the better is the cut quality. The burr has a higher weighting than the surface roughness, based on the priorities known from the daily industrial cutting business. The reference speed $v_{\text{reference}}$ amounts to 0.4 m/min and was determined by cutting trials with static beam shaping.

$$\text{performance} = 0.2 \frac{\text{criterion}_{R_z}}{4} + 0.5 \frac{\text{criterion}_{\text{burr}}}{3} + 0.3 \frac{v_{\text{reference}}}{v_c} \tag{2}$$

3 Results and discussion

The principle of laser beam fusion cutting is based on the interaction of laser radiation and material to generate a melt pool. The molten material is ejected by an inert gas jet with a pressure of up to 20 bar. A precondition of the melting procedure is the heat conduction of the material. Heating up a material with a Gaussian near energy distribution of the laser beam and low specific heat conduction of the processed material causes an inhomogeneous temperature distribution and, as a consequence, a highly dynamic melt pool. The static beam shaping does not influence the temperature gradient because the intensity distribution is still Gaussian. The melt pool dynamic could be only decreased by reducing the heat conduction effect by means of a shorter interaction time. The reason is that a longer interaction time causes energy accumulation and local vaporization, which result in a higher cut edge roughness. Obviously, a highly dynamic process like laser beam fusion cutting needs a highly dynamic beam-shaping method. The authors' idea is to work with a high intensity laser beam but minimized local interaction time to decrease melt pool turbulence and heat conduction losses. Precondition is the implementation of a highly dynamic scanner in the cutting equipment.

The experimental matrix investigates different frequencies, amplitudes, and phase shifts resulting in various *Lissajous* figures (circle, ellipse, horseshoe, and eight). The amplitude and frequency could optimize the heat conduction because they influence the beam velocity, which determines the interaction time and, therefore, the heat conduction and, in turn, could avoid the formation of heat accumulation. The amplitude itself affects also the cut kerf size. The oscillation pattern has a general impact on the local energy input as depicted in the beam measurements in Figure 4.

In the case of a circular beam oscillation, the laser beam interacts nearly homogenous to the cutting front. There is only a difference of the beam velocity vector between the left and right cut kerf wall because the

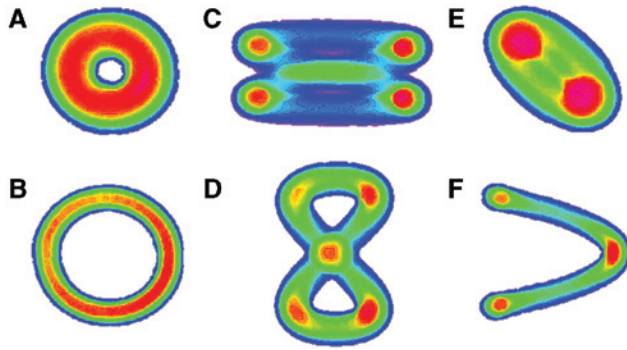


Figure 4: Beam measurement of different *Lissajous* figures, (A) and (B) $F_x:F_y=1, A_x:A_y=1, \varphi=90^\circ/270^\circ$, (C) and (D) $F_x:F_y=2:1, A_x:A_y=\text{arbitrary}, \varphi=0^\circ/90^\circ$, (E) $F_x:F_y=1:1, A_x:A_y=\text{arbitrary}, \varphi=180^\circ$, (F) $F_x:F_y=2:1, A_x:A_y=\text{arbitrary}, \varphi=22^\circ/225^\circ$.

rotational direction differs as illustrated in Figure 5. The pattern ‘8 perpendicular to the cut kerf’ has the same interaction time and rotational direction for the left and right cut edge.

Figure 6 contains the selected operating points in dependence of the *Lissajous* figure for both optical setups

and two possible demands: good quality or highest achievable cutting speed at tolerable quality. The included letters represent the cutting performance converted to the American grading system by means of Table 5.

The origin of the following discussion is the reference sample, created with the state-of-the-art static beam shaping. The reference feed rate is 0.4 m/min, and the cut quality is evaluated as mark D. In combination with the dynamic beam shaping, both setups increase the achievable cutting speed by about 30% as well as improve the cut quality. Thus, the efficiency of the cut process is enhanced. Setup 1 exhibits a wider range on reached cutting speeds in comparison to setup 2, which is almost constant even for the varying demands.

Hence, the available parameter range is more stable in the case of setup 1. The first result of the trials is a better cutting performance for setup 1, as expected, because the smaller focus spot provides higher intensities and, thus, improved absorption behavior, which influences the melt flow positively.

Both setups improved the cut quality. Each operating point of Figure 6 originates from a design of experiment

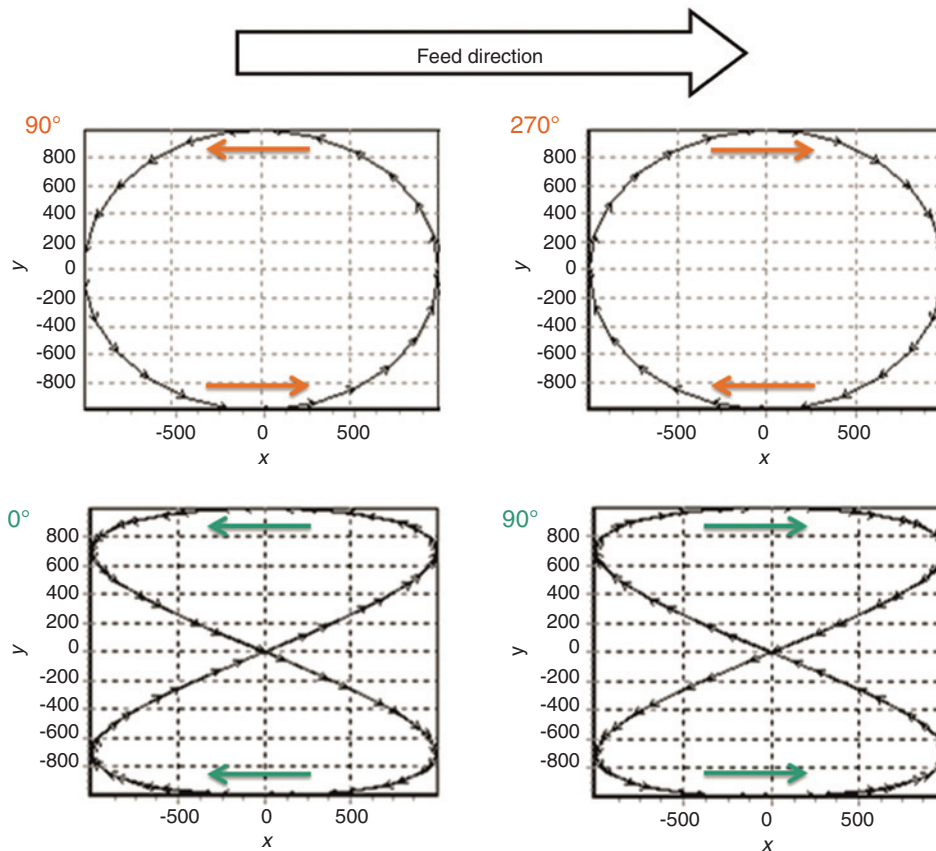


Figure 5: Rotational direction for *Lissajous* figure circle and ‘8 perpendicular to the cut kerf’; influence of phase shift to the velocity vector of the beam, relative to the feed direction.

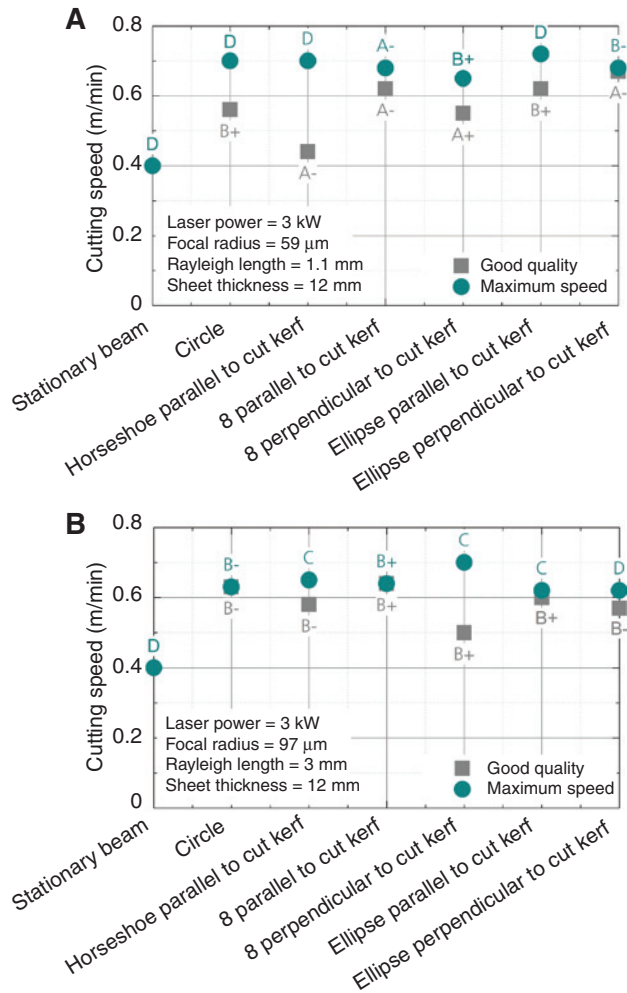


Figure 6: Cutting speed for different *Lissajous* figures in the case of good quality or maximum achievable feed rate for both optical setups and 12 mm stainless steel; (A) setup 1; (B) setup 2.

Table 5: Transformation of the performance criterion to the American grading system.

Mark	Performance criterion
A	Performance ≤ 0.5
B	0.5 < performance ≤ 0.7
C	0.7 < performance ≤ 0.9
D	Performance > 0.9

for each individual *Lissajous* figure. The discussion hereafter will state how the single criteria burr and surface roughness were influenced by the scanner parameters one time. For that purpose, the *Lissajous* figure with the best performance was chosen based on Figure 6. As the second outcome of the investigation, the pattern ‘8 perpendicular to the cut kerf’ performs the best cut. The dependency of scanner parameters and the quality criteria are illustrated

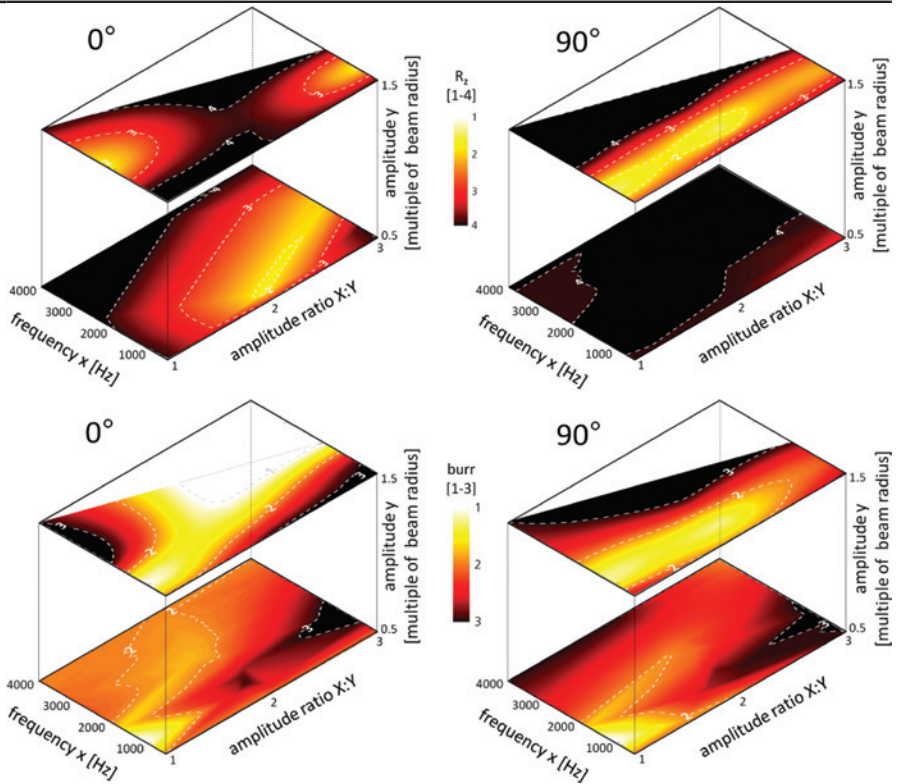
in Table 6 by means of area charts. Each cuboid represents the design of experiment. The pattern ‘8 perpendicular to the cut edge’ is determined by the frequency ratio $F_x:F_y=2:1$ and a phase shift of 0° or 90° . The distinction between the two phase shifts is attributed by the rotational direction of the *Lissajous* figure. The aim is to check if the rotational direction has an impact on the cut. Three more parameters are necessary for a complete description of the pattern: the frequency in the X direction, the amplitude in the Y direction, and the amplitude ratio $A_x:A_y$. The amplitude will be assigned as the multiple of the beam radius ω_0 in the focal plane. The beam measurements of Figure 4C and D are examples of the discussed beam shape. A full-factorial design of experiment is not possible because of the infinite scanner parameter combinations. The present trials attempt to accomplish the technical confinements of the scanner. These limitations are perceptible in the area charts below by the white marks. Especially, high frequencies combined with high amplitudes are not achievable.

In the case of setup 1, the surface roughness has one minimum at a frequency of 1 kHz, amplitude of $0.5\omega_0$, amplitude ratio of 2:1, and 0° phase shift. For 0° phase shift is the lowest burr height at a frequency of 2 kHz, amplitude of $1.5\omega_0$, and an amplitude ratio range from 2:1 to 3:1. There is no operating point that combines minima for both quality criteria. At 90° phase shift varies the circumstances. The optimal surface roughness and burr are both exhibited at a frequency of 1 kHz, amplitude of $1.5\omega_0$, and an amplitude ratio range from 1:1 to 2:1. Hence, at these adapted scanner parameters, there is a low surface roughness and coincident slight burr realizable. The phase shift 90° , the laser beam rotates toward the cut front, reaches better results in the case of setup 1. One possible explanation is the melt flow. The laser beam melts material on the kerf walls and acts as a force to transport the melt away from the generating cut edges at the same time, to avoid solidifications and consequently minimize the surface roughness.

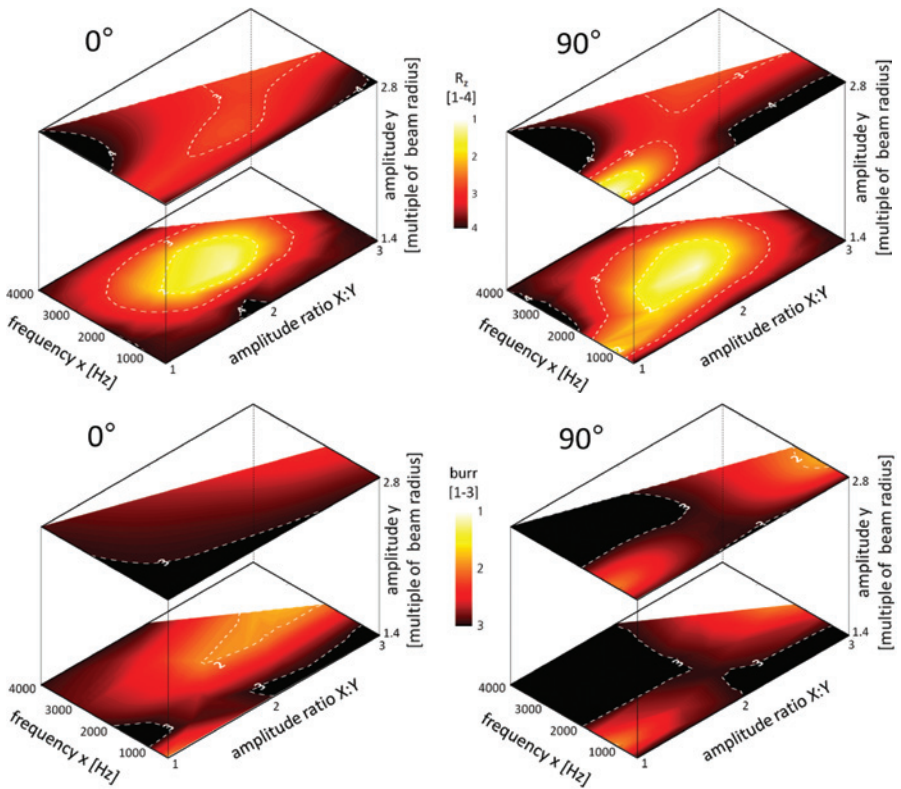
For the second setup, the phase shift has no significant influence on the resulting cut edge with respect to the quality criteria. The minimum surface roughness is reached at a frequency of 2.5 kHz, amplitude of $1.4\omega_0$, and an amplitude ratio of 2:1. The lowest burr height is independent of the amplitude. At small frequencies of about 1 kHz and an amplitude ratio of 1:1 or frequencies of 2 kHz and an amplitude ratio of 3:1, there are minima indicated. The entire location is not detectable because the limitations of the scanner are attained. The suggestion is to detect, so far, just local optima, which are also observed for setup 1. A statistical analysis of the trials outlines the frequency as the main influencing scanning parameter

Table 6: Overview of the criteria surface roughness, burr, and cutting performance in dependence of scanning parameters in the case of the *Lissajous* Figure ‘8 perpendicular to the cut kerf’ for both setups.

Setup 1 ($\omega_0=59 \mu\text{m}$, $z_R=1.1 \text{ mm}$)



Setup 2 ($\omega_0=97 \mu\text{m}$, $z_R=3 \text{ mm}$)



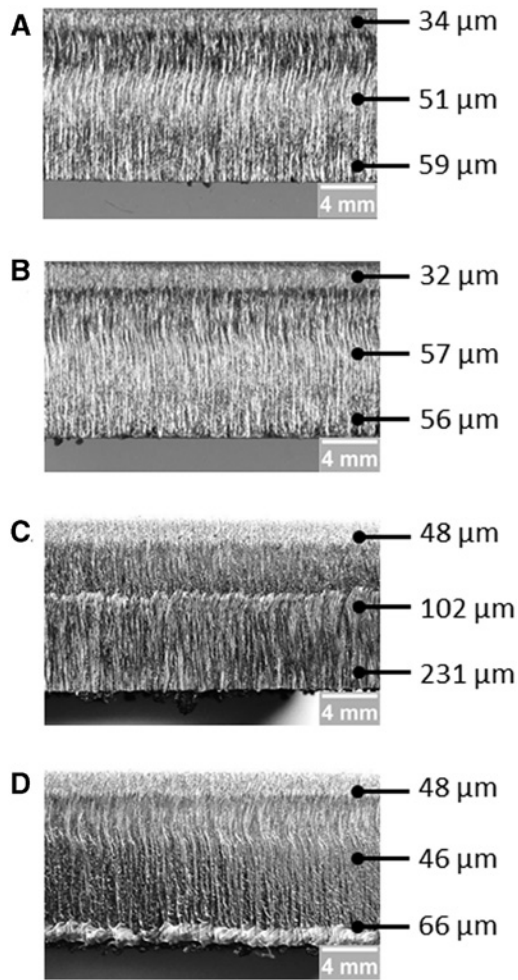


Figure 7: Cut edges of 12 mm stainless steel for (A) setup 1 combined with the dynamic beam shaping; (B) setup 2 combined with the dynamic beam shaping; (C) state-of-the-art cut with static beam shaping at 3 kW laser output power; (D) state-of-the-art cut with static beam shaping at 6 kW laser output power.

on the cutting performance. Hence, the expectation is to reach a global optimum with enhanced scanner technology that enables higher frequencies accompanied with higher amplitudes.

Setup 1 exhibits no clear dependency between surface roughness and burr height. At 0° phase shift are both criteria contrary. If the surface roughness is minimized, the burr will be increased and the other way around. The cuboids for 90° phase shift and a high amplitude value of $1.5\omega_0$ illustrate a straight correlation between surface roughness and burr. Setup 2 has some accordance regarding the position of the optima from the quality criteria. Especially for the lower frequencies is that perceptible in the cuboids.

The best cutting result for setup 1 utilizing the pattern ‘8 perpendicular to the cut kerf’ is achieved at a frequency in the X direction of 1 kHz, amplitude in the Y direction of $1.5\omega_0$, and an amplitude ratio of 1:1 by 90° phase shift. In the case of setup 2, the operating point is located at a frequency in the X direction of 2 kHz, amplitude in the Y direction of $1.4\omega_0$, and an amplitude ratio of 2:1 with a phase shift of 0° . These adapted scanner parameters optimize the surface roughness as well as the burr height compared with the reference samples. The sample cut with setup 1 combined with the scanner achieved for both quality criteria level 1 and 0.55 m/min cutting speed. This matches a performance of A⁺. The sample of setup 2 comes up with level 2 for the burr, level 1 for the surface roughness, and 0.5 m/min cutting speed that translates to a performance of mark B⁺. By way of illustration, the cut edges are depicted in Figure 7. The state-of-the-art reference sample is also included and, furthermore, a state-of-the-art sample cut with increased laser power up to 6 kW. The beam oscillation technology exhibits almost no

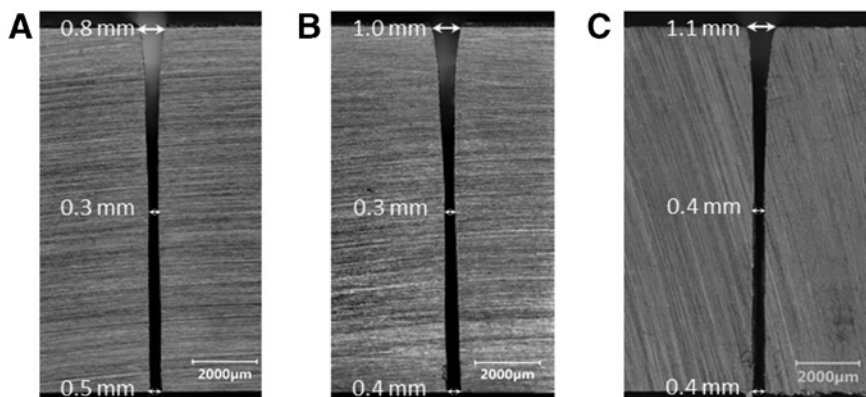


Figure 8: Cut kerf geometry of 12 mm stainless steel for (A) state-of-the-art cut with static beam shaping at 3 kW laser output power; (B) setup 1 combined with the dynamic beam shaping; (C) setup 2 combined with the dynamic beam shaping.

burr. The static beam at 3 kW laser output power effected higher surface roughness in the lower part of the cut edge. The reason is that the melt is not completely ejected. The increased laser power reached a similar surface roughness as the dynamic beam shaping. However, there are melt attachments visible on the lower cut edge.

The beam shaping, static as well as dynamic, influences mainly the cut kerf geometry. The surface roughness and burr are a consequence of the generated cut kerf. Figure 8 illustrates the differences between the beam shaping methods. Owing to the dynamic modification of the interaction zone of laser and material surface, the melt volume is slightly increased. The state-of-the-art cut with comparable power level has a cross-sectional area of the cut kerf of 4.5 mm^2 , whereas the beam oscillation reached 5.2 mm^2 for setup 1 and 5.4 mm^2 for setup 2. The enlargement of the cut kerf takes mostly part on the sheet top side and is just about 0.3 mm. Despite the increased interaction zone of laser beam and material, the cut kerf geometry has not significantly changed. However, one suggestion for the improved cutting performance of the dynamic beam shaping depends upon the increased kerf width on the top, where the laser beam as well as the gas jet enters the material. The gas efficiency is probably raised above the usual 30%, which is coupled into the cut kerf and improve the melt ejection.

Setup 1 is the most beneficial in the performed trials. The small focus spot with corresponding short *Rayleigh* length is usually applied for laser beam cutting of thin sheets. The scanner enables the further utilization of the high intensity and simultaneously is the beam modified into an arbitrary shape. The five additional parameters from the scanner can create an infinite quantity of artificial focal spots. Independent of that is the *Rayleigh* length always increased. From experience, the *Rayleigh* length should be in the range of the sheet thickness for quality cuts. The artificial increased *Rayleigh* length by the dynamic beam shaping entails an optical setup, recommended for thin sheets, to cut also thicker sheets. There is no more need to replace the optical configuration with changing cutting tasks.

4 Conclusion

The present investigation deals with the improvement of the performance in fiber laser cutting of thick stainless steel through beam oscillation technology. A mandatory precondition is a highly dynamic scanner for the two-dimensional working field. The utilized scanner reaches frequencies of up to 4 kHz, that is the technical

limitation for galvano-driven solutions. The present trials highlight the beam oscillation technology as a very promising method to improve the cutting performance for the thick material range. Two standard optical configurations combined with the dynamic beam shaping were compared regarding their cutting performance. The smaller focus spot achieves better results because the beam shaping creates a new artificial focal spot, which meets the requirements of the cutting process. The generated cut kerf is enlarged at the top side by which the gas jet is more capable, and the melt ejection improved. After all, the cut quality as well as the productivity is enhanced compared with the state-of-the-art cuts with static beam shaping. The *Lissajous* pattern ‘8 perpendicular to the cut kerf’ was discussed more in detail because of conspicuous good cutting results. Operating points are exhibited just as indications that the opportunity exists for a further improvement of the cut performance beyond the present confinements of the beam oscillation. Statistical analysis points out the frequency as the main influencing scanner parameter.

The investigation demonstrates advantages of a smaller focus spot, but there are also differences referring to the dependencies of the single parameters that are obvious between the two optical setups. The utilization of dynamic beam shaping is complex, and there is still a need for adaptations of all process conditions: optical setup, material, sheet thickness, laser parameter, scanner parameter, etc.

The challenges for the future will be, on the one hand, the evolution of a simulation model that enables forecasts of scanner parameter combinations to the cut result. Therefore, many more dependencies have to be clarified to detect universal coherences between other *Lissajous* figures, optical setups, work piece materials, etc. On the other hand is the development of new technologies for scanner drives that overcome today’s limitations.

However, the dynamic beam shaping in combination with a standard optical setup for thin sheets is able to cut thicker materials in good quality. The vision of an all-rounder cutting machine that can be adapted to every customer demand with just one optic is one step closer.

References

- [1] Optech Consulting, Press Release, 21st January 2015.
- [2] Optech Consulting, Laser Magazin, 2, 48 (2014).
- [3] G. Overton, A. Nogee, D. A. Belforte and C. Holton, Laser Focus World 49/1, 36–70, (2013).
- [4] Conzeta, Geschäftsbericht 2014.

- [5] Amada Group, Annual Report 2014.
- [6] Trumpf Gruppe, Geschäftsbericht 2014/15.
- [7] Prima Industrie, Facts and Figures 2014.
- [8] O. F. Olsen, Proc. of the 25th ICALEO, 188–196 (2006).
- [9] C. Wandera, PhD thesis (2010).
- [10] T. Himmer, T. Pinder, L. Morgenthal and E. Beyer, Proc. of the 26th ICALEO, 87–91 (2007).
- [11] W. O’Neill, The Laser User, Issue 51, 34–36, (2008).
- [12] R. Poprawe, W. Schulz and R. Schmitt, Physics Procedia, 5, 1–18 (2010).
- [13] P. A. Hilton, Proc. of the 5th LAMP (2009).
- [14] A. Mahrle and E. Beyer, Proc. of the 5th LIM 215–221 (2009).
- [15] A. Mahrle and E. Beyer, Proc. of the 28th ICALEO 610–619 (2009).
- [16] D. Petring, F. Schneider, N. Wolf and V. N. Goneghany, The Laser User, Issue 56, 20–23 (2009).
- [17] L. D. Scintilla, L. Tricarico, A. Mahrle, A. Wetzig, T. Himmer, et al. The Laser User, Issue 62, 24–26 (2011).
- [18] F. O. Olsen, Proc. of the 30th ICALEO, 6–15 (2011).
- [19] D. Petring, F. Schneider and N. Wolf, Proc. of the 31st ICALEO, 43–48 (2012).
- [20] D. Petring, T. Molitor, F. Schneider and N. Wolf, Physics Procedia 39, 186–196 (2012).
- [21] K. Hirano and R. Fabbro, J. Laser Appl. 24, 12006–12014 (2012).
- [22] K. Hirano and R. Fabbro, Proc. of the 32th ICALEO, 119–124 (2013).
- [23] L. D. Scintilla, L. Tricarico, A. Wetzig and E. Beyer, Int. J. Mach. Tool. Manu. 69, 30–37, (2013).
- [24] S. Stelzer, A. Mahrle, A. Wetzig and E. Beyer, Physics Procedia 41, 399–404 (2013).
- [25] A. Laskin, Technology report 2006, π Shaper.
- [26] Holo/Or Ltd, Web: http://www.holor.co.il/Diffractive_optics_Applications/Application_Notes_BeamShapers.htm (2013).
- [27] C. G. Gómez, Master thesis, Brno University of Technology, (2012).
- [28] O. F. Olsen, K. S. Hansen and J. S. Nielsen, J. Laser Appl. 21, 133–138, (2001).
- [29] C. Maclair, D. Pietroy, Y. D. Maïo, E. Baubeau, J. P. Colombier, et al., Opt. Lasers Eng. 67, 212–217 (2015).
- [30] J. Powell, W. K. Tan, P. MacLennan, D. Rudd, C. Wykes, et al., J. Laser Appl. 12, 224–231 (2000).
- [31] A. Mahrle and E. Beyer, J. Phys. D: Appl. Phys. 42, 175507–175516 (2009).
- [32] C. Goppold, K. Zenger, P. Herwig, A. Wetzig, A. Mahrle, et al., Physics Procedia 56, 892–900 (2014).
- [33] S. Schiller, U. Heisig and S. Panzer, ‘Elektronenstrahltechnologie’ (Verlag Technik GmbH, Berlin, 1995).
- [34] D. von Dobeneck, T. Löwer and V. Adam, ‘Elektronenstrahlschweißen – Das Verfahren und seine industrielle Anwendung für höchste Produktivität’ (Verlag Moderne Industrie, Landsberg/Lech, 2001).
- [35] K. Matthes and E. Richter, ‘Schweißtechnik’ (Fachbuchverlag, Leipzig, 2003).
- [36] J. Overrath, Dissertationsschrift, TU Braunschweig, 1998.
- [37] R. Schedewy, D. Dittrich, J. Standfuss and B. Brenner, Proc. of the 27th ICALEO, 332–339 (2008).
- [38] M. Krätzsch, J. Standfuss, A. Klotzbach, J. Kaspar, B. Brenner, et al., Physics Procedia 12, 142–149 (2011).
- [39] M. Schweier, J. F. Heins, M. W. Haubold and M. F. Zäh, Physics Procedia 41, 20–30 (2013).
- [40] C. Thiel, R. Weber, J. Johannsen and T. Graf, Physics Procedia 41, 209–215 (2013).
- [41] A. Müller, S. F. Goecke, P. Sievi, F. Albert and M. Rethmeier, Physics Procedia 56, 458–466 (2014).
- [42] K. Hao, G. Li, M. Gao and X. Zeng, J. Mater. Process. Technol. 225, 77–83 (2015).
- [43] T. Arai and S. Riches, Proc. of the 16th ICALEO, 19–26 (1997).
- [44] Y. Morimoto, D. He, W. Hijikata, T. Shinshi, T. Nakai, et al., Precision Eng. 40, 112–123 (2015).
- [45] J. Harris and M. Brandt, Proc. of the 20th ICALEO, section B, paper 1502, p. 1–8 (2001).
- [46] A. Mahrle, F. Bartels and E. Beyer, Proc. of the 27th ICALEO, 703–712 (2008).
- [47] C. Goppold, T. Pinder, P. Herwig, A. Mahrle, A. Wetzig, et al., LIM 2015.



Cindy Goppold

Fraunhofer IWS, Winterbergstraße 28, 01277
Dresden, Germany
cindy.goppold@iws.fraunhofer.de

Cindy Goppold is a research associate in the department Laser Ablation and Cutting at the Fraunhofer Institute for Material and Beam Technology IWS in Dresden, Germany. She earned her Master of Engineering in Laser- and Optotechnologies at the University of Applied Sciences Ernst-Abbe-Hochschule Jena, Germany. Her current research interests focus on the development of new approaches for the conventional laser beam cutting of metals.



Thomas Pinder

Fraunhofer IWS, Winterbergstraße 28, 01277
Dresden, Germany

Thomas Pinder is a research associate in the department Laser Ablation and Cutting at the Fraunhofer Institute for Material and Beam Technology IWS in Dresden, Germany. He studied Mechanical Engineering at the Technical University of Dresden, Germany. He gained competences in signal processing in the case of laser beam cutting over the last years.



Patrick Herwig
Fraunhofer IWS, Winterbergstraße 28, 01277
Dresden, Germany

Patrick Herwig studied Mechatronics to MSc degree. He received his PhD in Mechanical Engineering at the Technical University of Dresden, Germany. After 5 years of research activities in the field of System Technology, he takes the lead of the Laser Cutting group at Fraunhofer IWS. His team focuses on efficiency and quality improvements for conventional laser cutting processes and the development of new technologies like the laser remote cutting.